2-D Finite-difference Modelling of Pore-pressure Diffusion in Heterogeneous Anisotropic Porolelastic Media: Implications for Induced Microseismicity

David W. Eaton*

Department of Geoscience, University of Calgary, Calgary, AB T2N 1N4

eatond@ucalgary.ca

Summary

Pore-fluid pressure is an important factor for understanding the onset, distribution and termination of induced seismicity due to injection of fluids into the subsurface. Injection of pore fluid reduces the effective normal stress, and if the normal stress is reduced sufficiently then basic Mohr-Coulomb failure theory predicts brittle failure of the rockmass. A number of recent studies have incorporated this basic concept, using a probabilistic approach to describe the induced seismicity. This approach is appealing because it provides a simple physical model (diffusion) to predict the stimulated rock volume based on relatively few poroelastic parameters such as permeability, dynamic fluid viscosity and elastic moduli. The concepts are illustrated here with numerical simulations of pore-pressure diffusion in media where the permeability is anisotropic and inhomogeneous. An unexpected finding is that, based on poroelastic theory, calculated values for hydraulic diffusivity (the derived parameter that controls pore-pressure diffusion) for unconventional reservoirs are orders-of-magnitude smaller than empirical hydraulic diffusivity derived from microseismic monitoring data. This suggests that, while pore pressure is undoubtedly important and the diffusion model may well provide a useful mathematical description of processes that occur during and after injection, a poroelastic model to describe the medium may be oversimplified.

Introduction

Recent studies have highlighted the potential significance of pore-fluid pressure as a factor that may control the onset, termination and distribution of seismicity induced by fluid injection into the subsurface (e.g., Shapiro et al., 2003; Rothert and Shapiro, 2007; Shapiro and Dinske, 2009; Langenbruch and Shapiro, 2010). The basic concept behind the role of pore fluid pressure is illustrated in Figure 1, which shows a classic Mohr-circle diagram. The Mohr circle depicts the state-of-stress in a simplified manner: given principal stresses $\sigma_1 > \sigma_2 > \sigma_3$, the circle is drawn with its centre at:

$$\sigma_C = \frac{\sigma_1 + \sigma_3}{2} \qquad , \qquad (1)$$

with radius

$$\sigma_r = \sigma_1 - \sigma_3 \qquad . \qquad (2)$$

The axes of the graph represent the effective normal stress, σ_N, and the shear stress, τ. Every point on the circle describes the normal and shear stress state in the plane containing the σ_1 - σ_3 axes. The Coulomb-Navier failure criterion (e.g., Stacey and Davis, 2008) is:
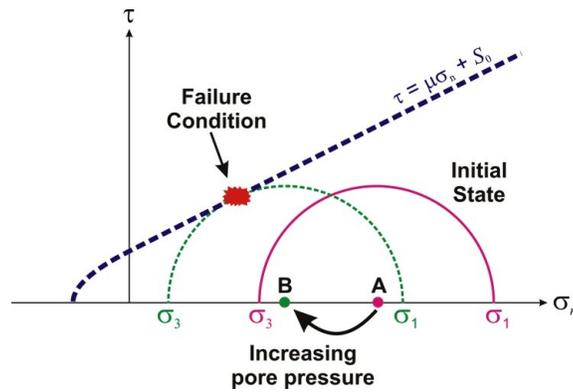
Figure 1: Mohr diagram showing the failure condition and effect of increasing pore-fluid pressure.

$$\tau = \mu\sigma_N + S_0 \qquad , \qquad\qquad (3)$$

where μ is the coefficient of friction and S_0 is called the internal cohesion. If the Mohr circle intersects the failure line, brittle failure of the rock occurs. The effect of fluid injection is to reduce the effective normal stress, i.e., in terms of the Mohr diagram, the Mohr circle shifts to the left. When the critical value of stress is achieved, failure occurs in the plane containing σ_2 and bisects the angle between σ_1 and σ_3 (Stacey and Davis, 2008).

The Earth rarely behaves in a clean and simple manner. Accordingly, a number of authors (e.g., Rothert and Shapiro, 2007; Langenbruch and Shapiro, 2010) have proposed a probabilistic approach in which rock failure is described by a finite probability [0-1] within a range of pore fluid pressure [C_{min} - C_{max}]. For pore-fluid pressures above C_{max}, failure is certain, whereas for pore fluid pressure below C_{min} there is no possibility of failure. An attractive feature of this approach is that pore-fluid pressure can be modeled as a diffusion phenomenon, facilitating meaningful predictions about induced seismicity on the basis of a relatively simple physical model. For example, using this approach Langenbruch and Shapiro (2010) model induced seismicity in a homogeneous poroelastic medium arising from a point injection source and show that microseismic activity occurs within a certain distance range from the source. In their model, r_{Cmin} defines the maximum distance away from the point of injection where failure can occur. With continued injection over time, diffusion theory predicts r_{Cmin} to increase; the stimulated rock volume thus slowly expands. An inner radius, r_{Cmax}, corresponds to the region where rock failure is certain. After termination of injection, pore fluid pressure relaxes back to an equilibrium state. This introduces a "back front", which represents the outward diffusion of the region where the pressure drops below C_{min}. Taken together, this model describes a volume of the subsurface where rock failure (induced seismicity) can occur.

The purpose of this paper is to illustrate these concepts of pore-fluid pressure diffusion using numerical simulations for an inhomogeneous poroelastic medium. Given the possibility that unconventional reservoirs are characterized by anisotropy, the numerical simulations are also performed using anisotropic properties.

Theory

In a porous medium, the diffusion of pore-fluid pressure is described by the diffusion equation (Shapiro et al, 2003)

$$\frac{\partial p}{\partial t} = \frac{\partial}{\partial x_i}\left[D_{ij} \frac{\partial}{\partial x_j} p(t,\mathbf{x}) \right] \qquad , \qquad (3)$$

where p is the pressure perturbation (generally the deviation from hydrostatic conditions), D_{ij} is the hydraulic-diffusivity tensor, and the summation convention is used. For a homogeneous anisotropic material the diffusion equation simplifies to

$$\frac{\partial p}{\partial t} = D_{ij} \frac{\partial^2}{\partial x_i \partial x_j} p(t,\mathbf{x}) \qquad . \qquad (4)$$

In a poroelastic medium, the hydraulic diffusivity is given by (Dutta and Ode, 1979)

$$\mathbf{D} = \frac{N\mathbf{K}}{\eta} \qquad , \qquad (5)$$

where N is a poroelastic parameter given by

$$N = \frac{MP_d}{H}; M = \left(\frac{\phi}{K_f} + \frac{\alpha - \phi}{K_g} \right)^{-1}; \alpha = 1 - \frac{K_d}{K_g}; H = P_d + \alpha^2 M; P_d = K_d + \frac{4}{3}\mu_d. \qquad (6)$$

The parameters in equation (6) are defined in Shapiro et al. (2003).

Example

The model parameters used for a suite of numerical simulations are given in Table 1. The hydraulic diffusivity values chosen for these simulations are generally of the same order of magnitude as those used by other workers for analytical solutions (e.g., Shapiro et al., 2003, Langenbruch and Shapiro, 2010). In each case, the computational grid contains 2000×500 points with a 1 m grid spacing and a time step of 1.0 s. The boundary condition $p = 0$ is imposed at the edges of the computational grid. An idealized scenario is considered with a point injection source at the centre of the grid [1000,250]. At the source point, a constant pressure perturbation is imposed at each time step for a period of 1800 s (i.e., 30 minutes) after which a pressure of $p = 0$ is imposed at the source point. Each simulation was run for 3000 time steps, in order to simulate the time period during and after injection. During the first 30 minutes of the simulation the injection pressure perturbation was assigned a value equal to hydrostatic pressure at 2600 m depth. Since this represents the perturbation to

Table 1. Parameters used for numerical modeling.

Model Number	D_{ij} (injection layer) [m²/s]	D_{ij} (background) [m²/s]
1	0.25	0.25
2	$\begin{bmatrix} 0.25 & 0 \\ 0 & 0.025 \end{bmatrix}$	$\begin{bmatrix} 0.25 & 0 \\ 0 & 0.025 \end{bmatrix}$
3	0.025	0.25
4	$\begin{bmatrix} 0.25 & 0 \\ 0 & 0.025 \end{bmatrix}$	$\begin{bmatrix} 0.15 & 0 \\ 0 & 0.1 \end{bmatrix}$
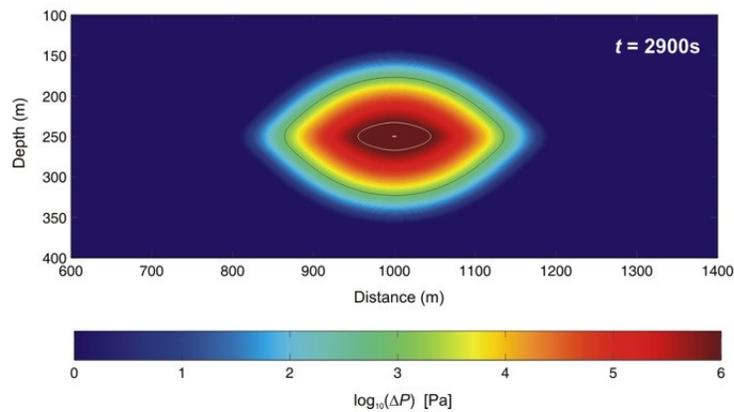
pressure, it corresponds to an injection pressure that is twice the hydrostatic pressure.

Figure 2: Snapshots of pressure perturbation for model 4. Black and white lines show outer and inner radii for seismicity.

Figure 2 shows a snapshot from the fourth simulation run, corresponding to fluid injection into a 50-m thick anisotropic layer than is more permeable in the horizontal direction than the layers above and below, but less permeable in the vertical direction. In this case, the predicted stimulated rock volume takes on an eye-like shape in two dimensions. Contours representing $C_{min} = 1$ kPa and $C_{max} = 1$ Mpa are shown for reference as black and white lines, respectively. These values of pressure perturbation correspond to those used by Langenbruch and Shapiro (2010) to represent the outer and inner radii of the stimulated rock volume, where the inner radius (r_{Cmax}) encloses the region of the subsurface where rock failure is certain based on their probabilistic model.

Conclusions

The numerical simulations presented here are based on 2-D finite-difference simulations of pore-pressure diffusion in anisotropic, inhomogeneous poroelastic media. They yield intuitively appealing examples that illustrate the manner in which pore-fluid perturbations might be expected to behave in the subsurface. Given probabilistic models for rock failure that have been proposed, such modeling could provide a simple basis for making predictions about stimulated rock volume. However, the empirical values of hydraulic diffusivity that appear to be necessary to explain the distribution of microseismicity induced by hydraulic fractures treatment (order of magnitude 1) are dramatically different from the hydraulic diffusivity predicted by poroelastic theory in a low permeability reservoir (order of magnitude 10^{-5}). This suggests that some other physical processes may need to be invoked to correctly describe the spatio-temporal behaviour of pore pressure diffusion in these types of rock materials.

Acknowledgements

References

Dutta, N.C. and Ode, H., 1979. Attenuation and dispersion of compressional waves in fulid-filled porous rocks with partial gas saturation (White model) – Part I: Biot Theory: Geophysics, **44**, 1777-1788.

Heidbach, O., Tingay, M., Barth, A., Reinecker, J., Kurfeß, D., Müller, B., 2009, The World Stress Map based on the database release 2008, equatorial scale 1:46,000,000, Commission for the Geological Map of the World, Paris, doi:10.1594/GFZ.WSM.Map2009.

Langenbruch, C. and Shapiro, S.A., 2010, Decay rate of fluid-induced seismicity after termination of reservoir stimulations: Geophysics, **75**, MA53-MA62.

Rothert E. and Shapiro, S.A., 2007, Statistics of fracture strength and fluid-induced microseismicity: Journal of Geophysical Research, **112**, B04, 309, doi: 10.1029/2005JB003959.

Shapiro, S.A., Patzig, R., Rothert, E. and Rindschwentner, J., 2003, Triggering of seismicity by pore-pressure perturbations: Permeability-related signature of the phenomenon: Pure and Applied Geophyscis, **160**, 1051-1066.

Shapiro, S.A. and Dinske, C., 2009, Scaling of seismicity induced by nonlinear fluid-rock interaction: Journal of Geophysical Research, **114**, B09, 2007, doi: 10.1029/2008JB006145.

Stacey, F.D. and Davis, P.M., 2008, Physics of the Earth (4th ed), Cambridge University Press, Cambridge, 532 pp.